

RESEARCH ARTICLE SUMMARY

NEUROSCIENCE

A global brain state underlies *C. elegans* sleep behavior

Annika L. A. Nichols, Tomáš Eichler, Richard Latham, Manuel Zimmer*

INTRODUCTION: Global brain states such as sleep and wakefulness involve reconfigurations of neural circuit activity across the entire nervous system. Yet it is not understood how the brain can effectively switch between and maintain different states. Do dedicated brain centers control states via top-down mechanisms? And to what extent do self-organizing principles of neuronal networks play a role? To address these questions, it would be ideal to measure the contributions of all individual neurons to a global brain state. Unfortunately, this is currently not possible in mammals or other large organisms. Every animal thoroughly studied exhibits sleep-like behaviors, implying that sleep is an essential, primordial, and common function of neural networks. In mammals, sleep is

defined at the physiological level by a characteristic electroencephalography (EEG) signal. Such a definition is missing for invertebrate models, which primarily rely on behavioral definitions.

RATIONALE: The nematode *Caenorhabditis elegans* is a tractable model organism with the potential to overcome these limitations: It has a stereotypic and mapped nervous system of only 302 neurons. Sleep is developmentally timed and occurs predominantly during lethargus periods of ~2 hours at the end of each larval stage. During wakefulness, the worm brain exhibits neuronal population dynamics that involve a large fraction (~40%) of neurons. These neuronal activities are highly coordinated across

the neuronal population; that is, they share common activity patterns. This feature can be quantified with computational methods and visualized in low-dimensional brain state phase plots. The resulting brain state trajectory represents the action sequence

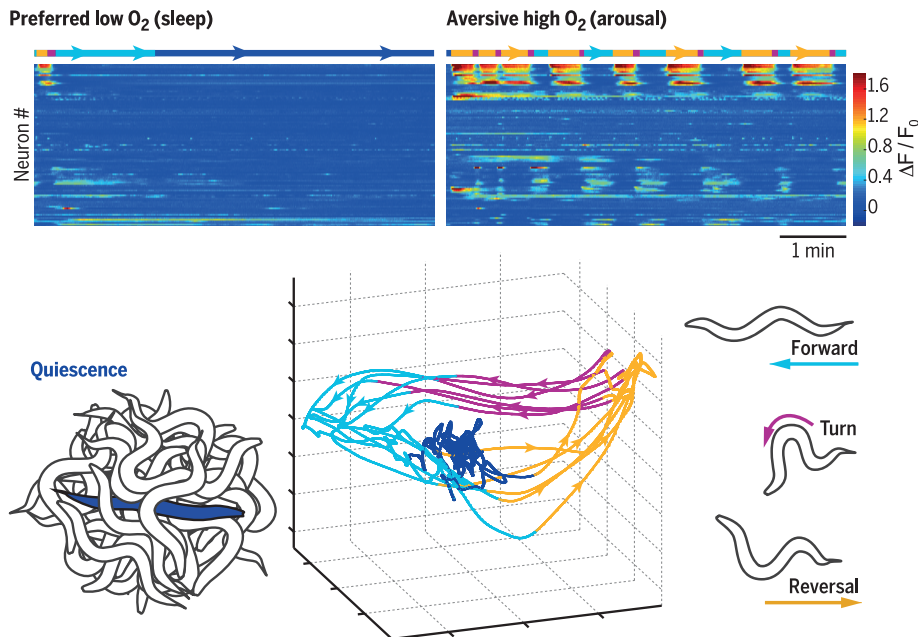
ON OUR WEBSITE

Read the full article at <http://dx.doi.org/10.1126/science.aam6851>

of the animals. To control sensory-evoked switching between sleep and wakefulness, we established a behavioral genetics paradigm combined with controlled changes in oxygen (O_2) concentration. This method, together with whole-brain imaging at single-cell resolution, enables us to observe brainwide neuronal activity dynamics during brain state transitions.

RESULTS: During lethargus, wild *C. elegans* strains prefer to sleep in social aggregates, and local O_2 concentrations are a key underlying cue. In this study, we have shown that a neuropeptide receptor (NPR-1) expressed in a hub interneuron regulates information processing of the arousal cue. We could recapitulate these switches between sleep and wakefulness in immobilized animals while recording the activity of nearly all neurons in the brain via Ca^{2+} imaging. We found that sleep in *C. elegans* is a global brain state in which about 75% of neurons displaying activity during wakefulness become inactive. However, a few specific neurons retained activity during sleep, notably γ -aminobutyric acid-producing (GABAergic) and peptidergic head neurons such as the sleep-promoting interneuron RIS. Chemosensory circuits activated by atmospheric O_2 rapidly evoked transitions to wakefulness by effectively activating neuronal population dynamics. In contrast, entries into sleep occurred spontaneously in the absence of arousing cues via convergence of neuronal activities toward the global quiescent state. Here, the sleep-active neurons retained stationary high activity.

CONCLUSION: Using computational analysis, we have shown that sleep is an emergent property of neuronal networks. When lethargus animals are in a favorable environment such as a social aggregate, sleep can evolve spontaneously in the absence of arousing cues; these, however, can rapidly reactivate dynamical brain activity. Our analysis reveals that neuronal networks feature properties of dynamic attractors during wakefulness, whereas during sleep these dynamics converge toward a fixed point. This attractor state mechanism could be a means to effectively switch between and maintain global brain states. ■



Sleep is a global quiescence brain state. Social aggregates of worms create a preferred milieu of low oxygen. During the lethargus developmental stage, these conditions permit sleep. Fluorescence heat maps (rectangles) show that wakefulness is associated with brainwide activity, whereas during sleep most neurons are down-regulated. The brain state cycles on a low-dimensional trajectory [as displayed by computational analysis (phase plot)], which corresponds to the pictured action command sequence. At sleep onset, these dynamics converge toward a tangle representing a fixed-point attractor state.

Research Institute of Molecular Pathology (IMP), Vienna Biocenter (VBC), Campus-Vienna-Biocenter 1, 1030 Vienna, Austria.

*Corresponding author. Email: manuel.zimmer@imp.ac.at
Cite this article as A. L. A. Nichols et al., *Science* 356, eaam6851 (2017). DOI: 10.1126/science.aam6851

RESEARCH ARTICLE

NEUROSCIENCE

A global brain state underlies *C. elegans* sleep behavior

Annika L. A. Nichols, Tomáš Eichler, Richard Latham, Manuel Zimmer*

How the brain effectively switches between and maintains global states, such as sleep and wakefulness, is not yet understood. We used brainwide functional imaging at single-cell resolution to show that during the developmental stage of lethargus, the *Caenorhabditis elegans* brain is predisposed to global quiescence, characterized by systemic down-regulation of neuronal activity. Only a few specific neurons are exempt from this effect. In the absence of external arousing cues, this quiescent brain state arises by the convergence of neuronal activities toward a fixed-point attractor embedded in an otherwise dynamic neural state space. We observed efficient spontaneous and sensory-evoked exits from quiescence. Our data support the hypothesis that during global states such as sleep, neuronal networks are drawn to a baseline mode and can be effectively reactivated by signaling from arousing circuits.

Behavioral states resembling mammalian sleep have been described across the Animalia phyla (1). The ubiquity of such observations suggests that some aspects of sleep observed in mammals might be fundamental to all nervous systems. Nonetheless, sleep is incompletely understood in terms of mechanism, regulation, and function. There are two major hypotheses concerning how this global brain state arises in the brain. One is a top-down regulatory mechanism implicating sleep-promoting centers in inducing sleep upon the rest of the brain (2). Alternatively, sleep onset may be a bottom-up mechanism, an emergent property of neuronal circuits, which is then spatially and temporally coordinated by sleep-regulatory circuits (3–6). Intriguingly, cultured mouse cortical neurons spontaneously display sleeplike activity but can be induced into wakelike activity by wake-promoting substances; this finding indicates that sleep may be the default state of neuronal networks (7). In mammals, there are cases in which behavior and local brain state are uncorrelated. For example, cetaceans such as dolphins can be awake and alert while their brains are sleeping unihemispherically (8). Furthermore, local cortical networks in awake rats can transiently go “offline” and display sleeplike properties (6). Similarly, subpopulations of Kenyon cells in *Drosophila* display sleeplike properties upon prolonged sleep deprivation (9). These studies highlight the need for comprehensively measuring the activity of local circuits and individual neurons across the entire brain to understand its global state.

Although great leaps in our understanding of neuronal activity during sleep have been made by recording local activity (6, 10–14) and global

activity at low resolution (15–18), currently available recording techniques do not have the spatial-temporal resolution to measure brainwide activity of single neurons in mammals. Therefore, we cannot determine how individual neurons across the entire brain are contributing to the emergent properties of global brain states.

The behavioral quiescence seen during the developmentally timed lethargus periods of the soil-dwelling nematode *Caenorhabditis elegans* has recently been shown to fulfill behavioral criteria for sleep [i.e., increased arousal thresholds (19), reversibility (19), specific posture (20–22), and homeostasis (19, 20, 23)]. During the lethargus stage, animals switch between behavioral quiescence (i.e., absence of any motion) and short, spontaneous periods of motion (19, 20). Furthermore, there is wide molecular conservation of regulation, including control of timing during development via PERIOD (which regulates circadian timing in other organisms); wakefulness-promoting signaling via pigment-dispersing factor (PDF), cyclic adenosine monophosphate (cAMP), and dopamine; and quiescence-promoting signaling via epidermal growth factor (EGF) (24–28). The γ -aminobutyric acid-producing (GABAergic) and peptidergic interneuron termed RIS has been shown to exhibit elevated activity during lethargus and to induce immobility when activated optogenetically (29). Furthermore, both sensory and downstream neurons have been shown to have dampened activity during quiescence (30–32). However, a comprehensive view of global nervous system activity changes during behavioral quiescence with single-cell resolution has been lacking.

Low-O₂ environments promote behavioral quiescence in *npr-1* animals

We first sought to establish an experimental paradigm for effective switching between quiescent and aroused brain states. Previous reports suggest

that during the domestication of the standard laboratory strain N2, several mutations were acquired and fixed in its genome (33). One of these mutations is a gain-of-function mutation in the G protein-coupled receptor *neuropeptide receptor 1* (*npr-1*) (34). All true wild *C. elegans* isolates tested so far have a low-activity allele of *npr-1*, called *g320* in the wild strain Hawaiian (33). These animals, as well as animals containing an *npr-1* loss-of-function mutant (*ad609*) in the N2 background (henceforth *npr-1* animals), accumulate at the border of bacterial lawns, where food is enriched. Here, they feed in groups by forming social aggregates, whereas standard N2 animals exhibit solitary feeding behavior. Therefore, the behavior of *npr-1* animals often serves as a proxy for behavior of wild strains (33, 34). Previous behavioral studies on animals in the lethargus period have reported that *npr-1* animals and wild strains have low levels of behavioral quiescence relative to N2 animals (25). However, when animals are left unperturbed in highly controlled environments for an extended time, *npr-1* shows only slightly less quiescence relative to N2 (23, 35). Because these studies were done on isolated animals, we aimed to measure the quiescence of animals in groups. We generated transgenic *npr-1* animals with fluorescent pharynges to easily detect and video-track individuals in social aggregates (Fig. 1, A and B, fig. S1A, and movie S1). We found that lethargus [as described in this study, representing late larval stage 4 (L4)] *npr-1* animals within social aggregates show periods of locomotor quiescence, whereas animals in the mid-L4 stage (prelethargus) generally do not. The same difference in activity between lethargus and prelethargus animals was seen for isolated *npr-1* animals that dwell in the bacterial border (Fig. 1B and fig. S1B). Thus, lethargus *npr-1* animals exhibit quiescence behavior in aggregates and bacterial lawn borders.

Low O₂ tension is one of the key environmental features found in both bacterial lawn borders and social aggregates (36, 37). To test whether O₂ levels alone could permit quiescence in *npr-1* animals, we modified a previously reported behavioral assay in which worms were placed in an O₂ flow arena for direct video tracking (38, 39); behavior was observed on a homogeneous food lawn lacking borders. The animals were kept at 21% (atmospheric) O₂ for 10 min, then shifted to 10% O₂, which is within the preferred concentration range of *npr-1* animals (36), for 10 min. This assay enables quantitative imaging of behavior, so that we could apply stringent criteria for defining quiescence versus active behavior—that is, prolonged absence versus occurrence of detectable movement such as locomotion or head motions (fig. S1, C to I, and supplementary materials). We found that prelethargus and lethargus *npr-1* animals were seldom quiescent at 21% O₂, which is consistent with the studies on isolated animals. At 10% O₂, only a few short bouts of quiescence could be observed in prelethargus *npr-1* animals; however, lethargus *npr-1* animals displayed long quiescence intervals with short interrupting bouts of activity

Research Institute of Molecular Pathology (IMP), Vienna Biocenter (VBC), Campus-Vienna-Biocenter 1, 1030 Vienna, Austria.

*Corresponding author. Email: manuel.zimmer@imp.ac.at

(Fig. 1, C and D). This motion pattern, referred to as lethargic behavior, was described previously in lethargus N2 animals (19, 20).

For all subsequent behavioral experiments, we established a high-throughput assay that allowed us to track individuals by video in populations of ~150 animals per assay, spanning the 10- to 12-hour period during which animals develop from the L4 prelethargus to the young adult stage under controlled O₂ environments. At constant 10% O₂, populations of *npr-1* animals were enriched in quiescent animals around the L4-to-adult transition (fig. S1J). We found that shifting the O₂ concentration to 21% for 6 min rapidly aroused all lethargic *npr-1* animals in a sustained manner (Fig. 1, E and F, and fig. S1K). The wild strain Hawaiian, like animals bearing the Hawaiian *npr-1(g320)* allele in the N2 genetic background, showed a similar response (Fig. 1, E and F). Conversely, lethargic N2 animals could only transiently be aroused in this paradigm (Fig. 1E). N2 populations kept at either constant 10% O₂ or constant 21% O₂ had nearly identical quiescence profiles, showing that the N2 lethargus quiescence is robust to these O₂ tensions (fig. S1, L and M). Next, we leveraged the O₂ stimulation paradigm to induce controlled periods of sleep deprivation

and found that the longer the time of sleep deprivation, the greater the fraction of the population in quiescence (fig. S2A) as well as the greater the fraction of time each animal was found quiescent (fig. S2B), both indicating homeostasis. Moreover, lethargus behavior at 10% O₂ was associated with increased arousal thresholds (fig. S2, C to H). Both observations support our interpretation that quiescence during the lethargus phase at 10% O₂ is a sleep state, as was previously shown for lethargus at uncontrolled O₂ tensions (19–23). These results imply that atmospheric O₂ levels (21%) cause sustained arousal during lethargus in a wild strain and in *npr-1* animals, whereas low-O₂ environments permit quiescence behavior like that reported for N2 animals.

O₂ sensory neurons and RMG hub interneurons are part of a neural circuit for arousal maintenance

To determine where this state-switching signal enters the nervous system, we tested genetic cell-ablation strains of previously identified chemosensory neurons involved in O₂ upshift sensing [AQR, PQR, and URX (38)] and downshift sensing [BAG (38)]. AQR, PQR, and URX, as well as a sol-

uble guanylate cyclase homolog [*gcy-35(ok769)*], are required for O₂ sensation in these cells (36, 38) and were required to arouse *npr-1* animals in a sustained manner at 21% O₂ (Fig. 2, A and B). Ablating BAG had no effect on arousal (Fig. 2B). In the absence of these cells or functional *gcy-35*, a transient arousal response to O₂ upshift remained, indicating a previously undescribed sensing mechanism for O₂ upshift (Fig. 2A and fig. S3A).

To identify the site of *npr-1*-mediated modulation, we performed transgenic rescue experiments. As a positive control, we expressed the N2 gain-of-function allele of *npr-1* from its endogenous promoter and could show full restoration of N2-like behaviors in *npr-1* animals (Fig. 2, C and D). Previous work showed that *npr-1* expression in the hub interneuron RMG is sufficient to promote solitary behavior (40). RMG is a gap junction hub connecting many sensory neurons (including URX) and interneurons (41) (fig. S4). We found that *npr-1* is required partially in the interneuron RMG to repress sustained arousal in response to 21% O₂ (Fig. 2, C to F), but not in the O₂ upshift sensory cells or the principal URX interneuron target AUA; there was no significant additive effect when combining with URX, AQR, and

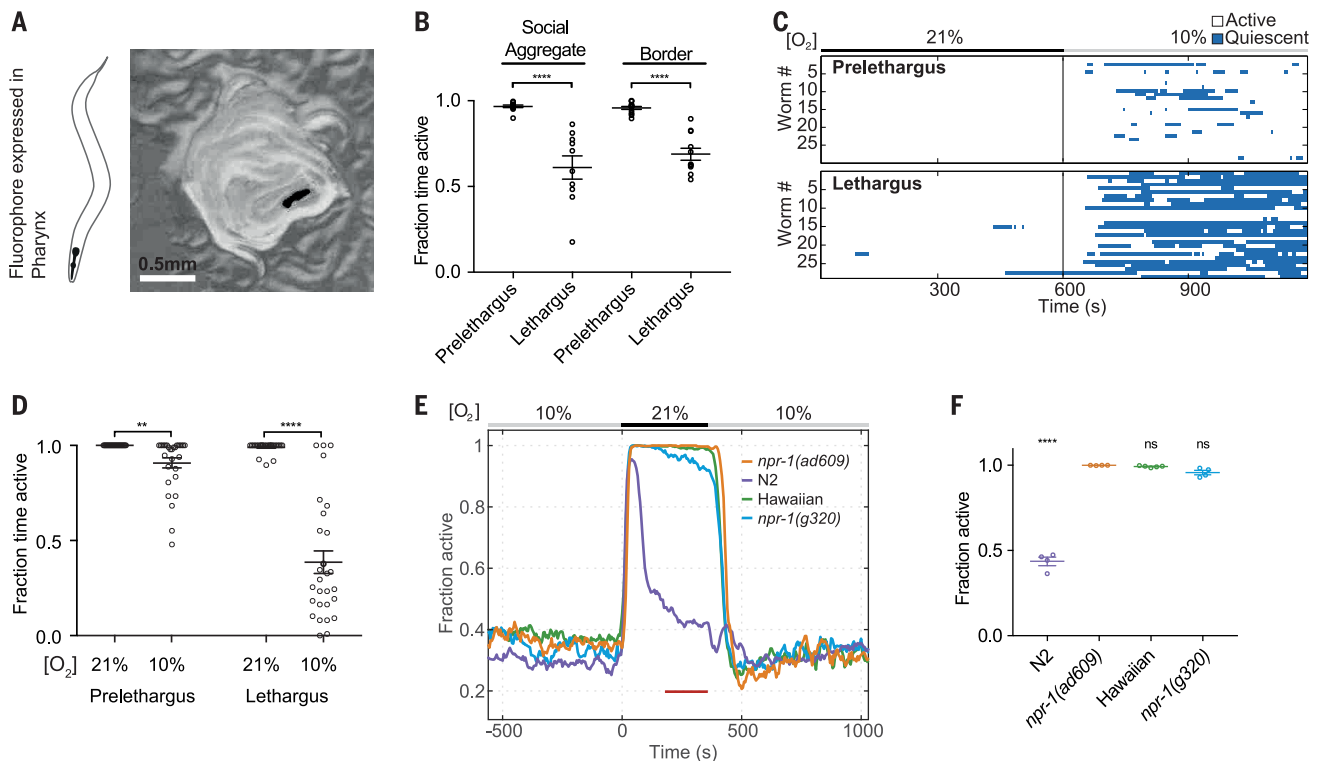


Fig. 1. Low-O₂ environments promote quiescence in *npr-1* animals.

(A) Left: Schematic of a worm expressing tdTomato fluorophore in the pharynx. Right: Inverted grayscale image (fluorescence + transmitted light) of a transgenic *npr-1* animal in a social aggregate of *npr-1* animals. (B) Quantitation of quiescence behavior during social aggregation and bordering of *npr-1* animals. Dots represent single animals; bars are means ± SEM (two-tailed *t* test). (C) Ethograms of behavioral state as defined by motion parameters (see fig. S1 and supplementary materials). (D) Quantitation of data in (C) from either the 21% O₂ or 10% O₂ periods.

Dots represent single animals; bars are means ± SEM (paired two-tailed *t* test). (E) Traces show average fraction of lethargic animals with the indicated genetic backgrounds responding to 6 min of 21% O₂; *g320* is the Hawaiian *npr-1* allele in the N2 background. (F) Quantitation of behavioral response during the period indicated by the red bar in (E). Dots show mean population response of lethargic animals for single experiments; bars are means ± SEM. Comparisons to *npr-1(ad609)* were made with a one-way analysis of variance (ANOVA) with Dunnett multiple-comparisons test. For all tests, ***P* < 0.01, *****P* < 0.0001; ns, not significant.

PQR or with AUA (Fig. 2, C and D). These results were consistent when tested in independent transgenic lines (fig. S3B). Furthermore, as previously described (40), endogenous *npr-1* expression as well as specific rescue in RMG restored solitary behavior (fig. S3C). We were not able to identify the remaining important *npr-1*-expressing cells with available promoter expression constructs.

Are there other modulatory inputs into the RMG circuit? To address this question, we first tested mutants for the known NPR-1 ligands but observed only a small effect on 21% O₂-induced arousal during lethargus (fig. S5, A and B). This is consistent with similarly small effects on aggregation behavior (42) and suggests additional yet unidentified NPR-1 ligands or the possibility that the N2 *npr-1* allele has constitutive activity. We also tested the involvement of the neuro-

peptide PDF and its receptors, which were reported to genetically interact with the *npr-1* pathway and are required for *npr-1*-mediated elevation of locomotor activity (25). Using our assay, we found that PDF signaling is required specifically for 21% O₂-evoked high-speed locomotion of *npr-1* animals but not for 21% O₂-evoked arousal from quiescence (fig. S5, C to H).

These findings imply the existence of a sensory circuit including primary oxygen sensors (URX, AQR, or PQR) and the RMG hub interneurons, which contribute to environment-dependent switching between active and quiescent behavioral states during lethargus.

Whole-brain imaging recapitulates lethargic behavior

Having established an experimental paradigm to rapidly switch between aroused and quiescent

behavioral states, we next sought the underlying neurological basis. We applied a recently reported brainwide Ca²⁺-imaging approach using a nuclear localized and pan-neuronally expressed Ca²⁺ indicator to record the activity of most head ganglia neurons at single-cell resolution (43, 44). In this approach, single animals are imaged while immobilized in microfluidic devices that allow for tight control over environmental O₂ levels (38). Using this approach, we previously reported on neuronal population dynamics in the brains of adult N2 animals and showed that the brain state, despite the immobilization condition, transitions through a cyclical sequence of motor command states (forward crawl, backward crawl, dorsal or ventral turn, forward crawl, etc.). These dynamics involve a large fraction (~40%) of all neurons in the brain, and each motor command state can be described by characteristic,

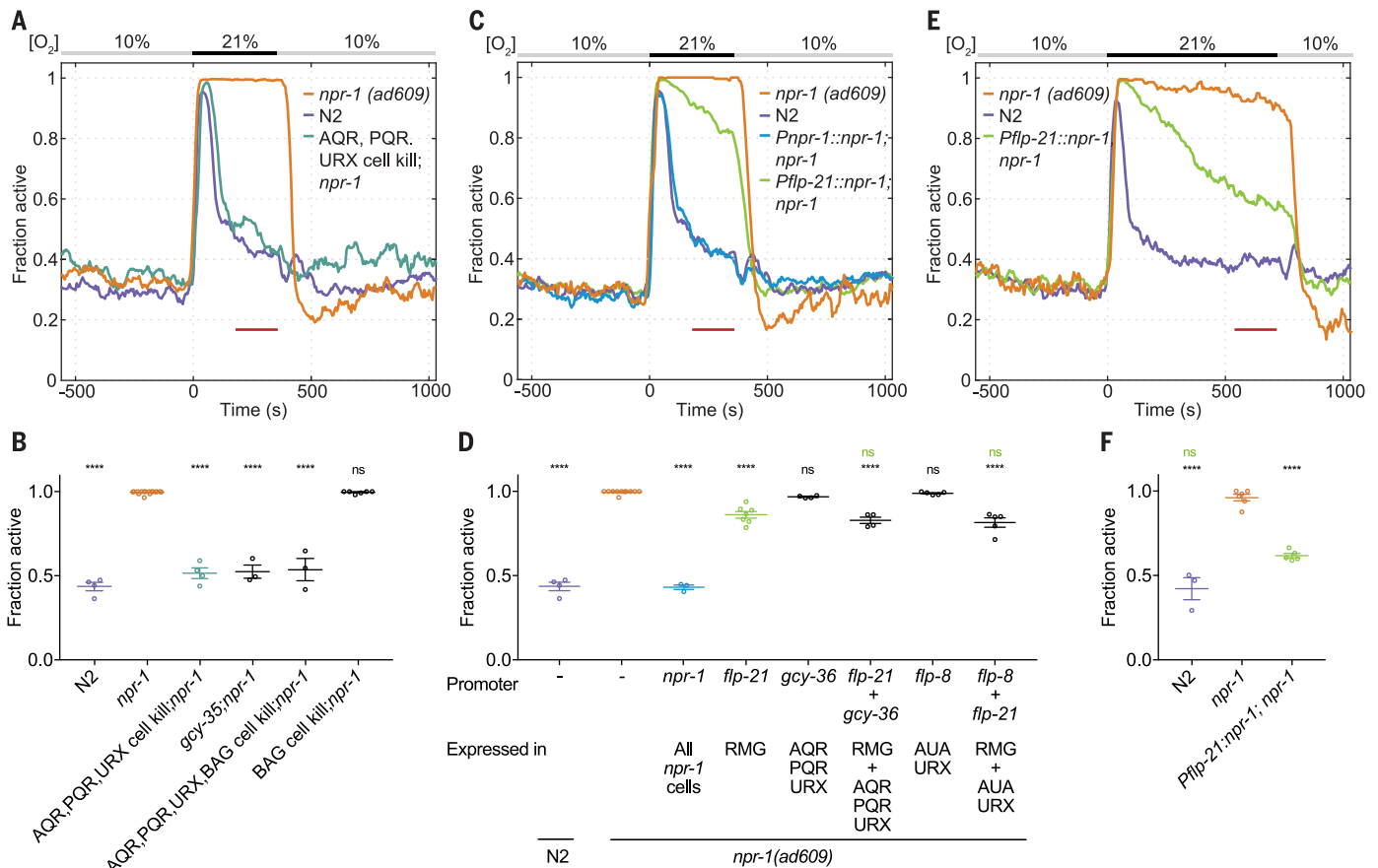


Fig. 2. O₂ sensory neurons and RMG hub interneurons are part of a neural circuit for arousal maintenance. (A) Traces show average response of lethargic animals with the indicated genetic backgrounds to 6 min of 21% O₂. AQR, PQR, URX cell kill; *npr-1* (i.e., genetic ablation); *npr-1* refers to *npr-1* animals in which AQR, PQR, and URX neurons have been ablated. (B) Quantitation of behavioral responses during the period indicated by the red bar in (A). (C) Average response of lethargic *npr-1(ad609)* animals to repeated exposure to 6 min of 21% O₂, rescued with either a *Pnpr-1::npr-1* (blue) or *Pflp-21::npr-1* (green) transgene and indicated control strains. (D) Quantitation of behavioral responses of transgenic rescues of *npr-1* during the period indicated by the red bar in (C). Cells that overlap between the rescue promoter and *Pnpr-1* are shown

below. (E) Same as (C) but with stimulus duration of 12 min. (F) Quantitation of behavioral responses during the period indicated by the red bar in (E). In (B), (D), and (F), dots indicate mean population response of lethargic animals for single experiments; bars show means ± SEM. N2 data in (A) to (D) are replicates from Fig. 1, E and F, for visualization purposes only. Comparisons to *npr-1* in (B) were made using a one-way ANOVA with Dunnett multiple-comparisons test. Comparisons between all indicated genetic backgrounds in (D) and (F) were made with a one-way ANOVA with Tukey multiple-comparisons test. For all statistical tests, *****P* < 0.0001. Black symbols indicate significance levels relative to *npr-1*; green symbols indicate significance levels for selected comparisons to *npr-1*; *Pflp-21::npr-1* rescue.

phasic, neuronal ensemble activities (44). We assayed *npr-1* and N2 animals in the presence of bacterial food at either the prelethargus or lethargus stage ($n = 10$ to 12 different individuals for each condition); a typical recording encompassed 80 to 130 neurons, of which the cell class of 20 to 41% could be identified. The stimulus reiterated a segment of the protocol used for the behavioral population assays (6 min

of 10% O₂, 6 min of 21% O₂, 6 min of 10% O₂) (Fig. 3 and movie S2). Prelethargus N2 and *npr-1* animals displayed the typical neuronal population dynamics at both 10% and 21% O₂ levels; lethargus N2 and *npr-1* animals in addition displayed periods of widespread down-regulation of brain dynamics at 10% O₂ (Fig. 3 and movie S2). Only *npr-1* animals were effectively aroused in all recordings by the 21% O₂ stimulus (Fig. 3D).

For subsequent quantitative analyses of these observations, we first established a classifier for the quiescent brain state periods. We defined quiescence by the absence of motor-related activity as defined by readings from AVA/L/R interneurons and SMDDL/R, SMDVL/R, VB, and RIVL/R motor neurons (most neuronal classes are represented by a left and a right member, specified by appending L or R, respectively). The

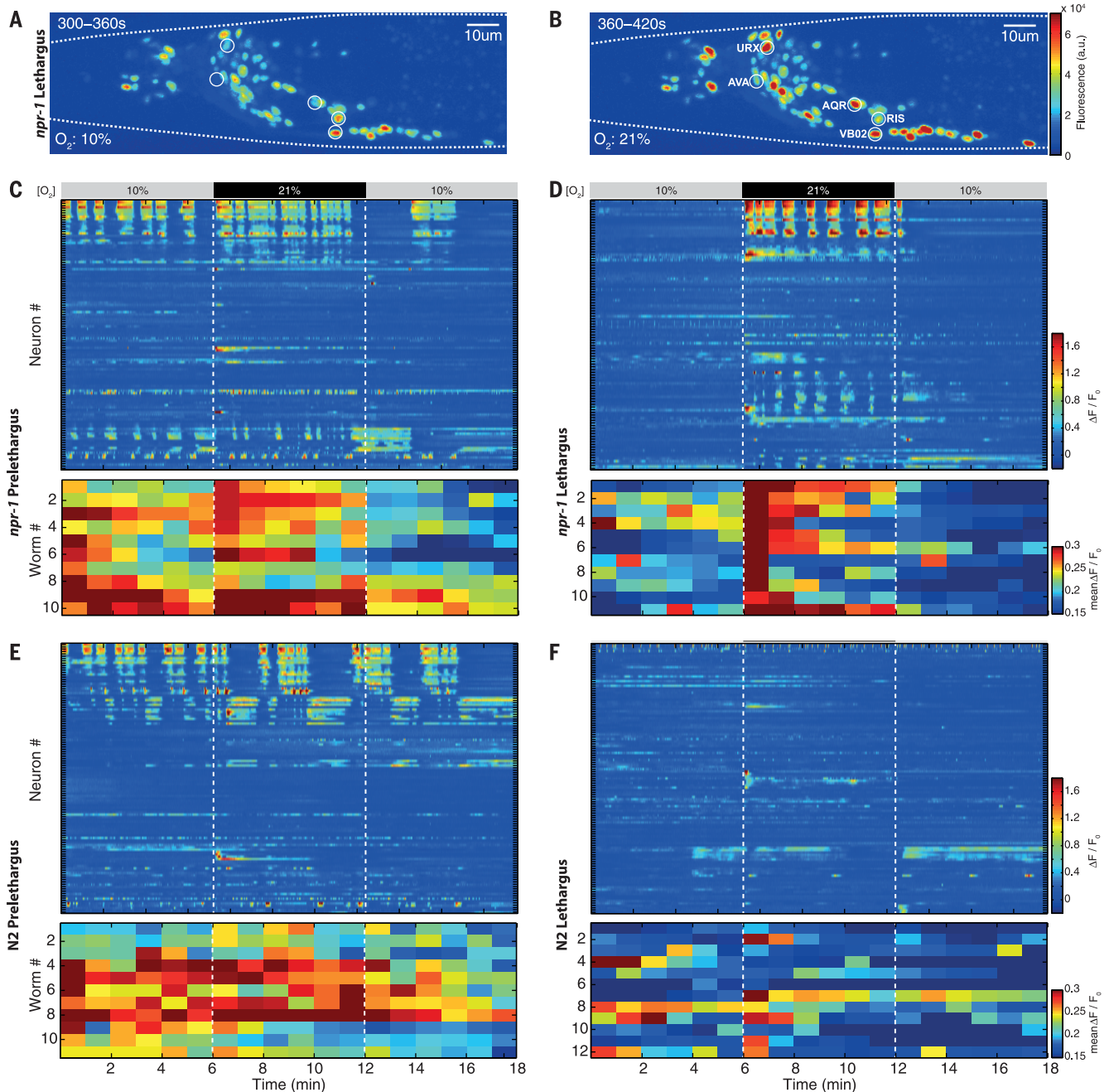


Fig. 3. Brainwide imaging of lethargus animals uncovers periods of widespread neuronal down-regulation. (A and B) Maximum-intensity projections of a brainwide imaging recording [same as in (D), upper panel], calculated across the indicated time periods. Identities of selected neurons are labeled. (C to F) Top: Examples of 18-min-long brainwide imaging recordings, shown as heat maps of fluorescence ($\Delta F/F_0$) time series of all

detected head ganglia neurons (one neuron per row, grouped by correlation and clustering). The O₂ stimulation protocol is indicated. Bottom: Global mean $\Delta F/F_0$ across all detected neurons (1-min binning) of each single recording in this study; each row is a different animal. Genotype and developmental stage are indicated. The first row is the recording in the respective upper panel.

activity of these neurons in freely behaving worms corresponds to the execution of one of the motor command states (44, 45) (Fig. 4, A and B, and fig. S6) (see supplementary materials for details). Prelethargus animals had very few periods of quiescence, whereas both N2 and *npr-1* lethargus animals displayed quiescence at baseline 10% O₂ (Fig. 4, C and D), like the levels seen in our behavioral assays (Fig. 1E). Furthermore, all *npr-1* lethargus animals exited quiescence when shifted to 21% O₂ and on average maintained the active state for the duration of the 6-min stimulus (Fig. 4C). Consistent with our behavioral results (for controls of transgenic lines, see fig. S7, A and B), the fraction of lethargus N2 animals in an active brain state transiently increased upon O₂ upshift (Fig. 4D). These data show that our results obtained in the behavioral paradigm can be recapitulated by whole-brain imaging in immobilized animals.

Quiescence during lethargus is a global brain state

We next quantified how the above-defined quiescence state correlates with global neuronal activity levels by calculating the mean cumulative frequency distributions of the change in fluorescence intensity ($\Delta F/F_0$) across all neurons (except neurons that encode O₂ sensory information). According to a $\Delta F/F_0$ cutoff for defining active versus inactive neurons during the aroused state in either prelethargus or lethargus animals, ~40% of all neurons were active; this number dropped to ~10% during quiescence in both lethargus N2 and lethargus *npr-1* animals (Fig. 4, E and F). Thus, during quiescence, about three-fourths of all neurons that are normally found to be active were down-regulated.

To investigate this observation further, we focused our subsequent analyses on all neurons from cell classes that could be reproducibly identified in enough recordings ($n \geq 3$). For example, the RIM and AVB interneurons, which are active during the reversal and forward motor command states, respectively (44), were both found to be largely inactive during quiescence (Fig. 4, G and H). We made the same observation for the gross majority of the other neurons belonging to the reversal or forward ensembles (Fig. 4, I and J). Also, a large fraction of neurons whose activity was not exclusive to the forward or reversal states was significantly down-regulated during quiescence; notable among these were sensory neurons that show spontaneous activity during active brain states (Fig. 4K). In summary, quiescence during lethargus affects many neurons of both the sensory and premotor domains.

Npr-1 animals exhibit an enhanced sensory-motor transformation

How could *npr-1* control the arousal thresholds of animals? To address this question, we interrogated our data for possible correlations between sensory circuit activity and genotype, developmental stage, or brain state. Mechanosensory and nociceptive neurons exhibit weaker sensory responses during lethargus in N2 animals but not

in *npr-1* animals (25, 30–32). In agreement with this, *npr-1* had nearly identical O₂-evoked responses in URX and AQR in prelethargus versus lethargus, but N2 had a larger variability in URX responses during lethargus, with some neurons not responding (fig. S8, A and B). Lethargus *npr-1* animals showed increased URX peak responses relative to lethargus N2 animals (fig. S8B). Although URX peak responses correlated with transient arousal (0 to 1 min after stimulus), we did not find such a correlation with sustained arousal (3 to 6 min after stimulus) (fig. S8, C and D). However, N2 AQRs responded similarly in prelethargus versus lethargus. Neither transient nor tonic responses in AQR (46) correlated with transient or sustained arousal (fig. S8, E to I). In summary, we did not find a striking modulation of AQR and URX that could explain the sustained arousal phenotype of *npr-1* animals.

We found that *npr-1* animals might have more complex O₂ sensory representations than N2, as we more frequently observed responses from AUA (a principal interneuron target of URX) and RMG interneurons (fig. S9, A and B). Moreover, we found more putative IL2 sensory neuron responses to O₂ upshift in *npr-1* animals (fig. S9C). O₂ sensory activity in IL2s, or in any other neuron in the anterior ganglion, has not been reported previously.

How do motor behavior-related brain dynamics change in response to the stimulus? The frequency of reversal command states, which corresponds to the frequency of cycles through the motor command sequence, was up-regulated at 21% O₂ in *npr-1* animals but not in N2 animals (fig. S10), showing that in comparison to N2, *npr-1* animals exhibit a more effective sensory-motor transformation in both prelethargus and lethargus stages. This is consistent with findings in adult animals (47). This effect could be caused by a more complex sensory representation of O₂ stimuli. As *npr-1*-mediated sustained arousal can be rescued in RMG neurons, RMG modulation might dampen the excitability of sensory circuits in an *npr-1*-dependent manner, preventing O₂-evoked sustained motor dynamics in N2 animals.

Quiescence displays features of a fixed-point attractor in neuronal population dynamics

We next focused our analysis on the neurons that were exempt from down-regulation during quiescence. Most prominent among these was the GABAergic and peptidergic sleep-active interneuron RIS, which exhibited Ca²⁺ plateaus during the forward state and remained active during quiescence (Fig. 4, B, L, and M); this observation is consistent with previous RIS recordings at low temporal resolution in unconstrained animals (29). Relative to prelethargus animals, RIS activity is elevated during the forward period in lethargus animals, which suggests that elevated RIS activity increases the likelihood of entering the quiescent state and that RIS activity during the forward state may reflect sleep pressure (Fig. 4, L and M). Besides RIS, other GABAergic head neurons such as RMED and RMEV, which

are active during the forward state (44) (Fig. 4, A and I, and fig. S11), showed residual (i.e., reduced-amplitude) Ca²⁺ plateaus during quiescence. This is consistent with increased GABA signaling during mammalian sleep (2). Similarly, the neuropeptidergic GABA uptake neuron ALA, which is required for stress-induced quiescence in adults (26, 48–50), showed some spontaneous activity and was not down-regulated during quiescence (Fig. 4K). In addition, the GABA uptake neuron AVF (50) was only slightly down-regulated during quiescence (Fig. 4K). Thus, although RIS, RMED, and RMEV decrease activity when the brain transitions from forward into a reversal state (44), they maintain tonic (i.e., sustained) activity when the system transitions into the quiescent state.

We next sought to characterize how quiescence is embedded in the neuronal population dynamics, where activities of subpopulations of neurons move through the motor command cycle described above (i.e., forward crawl, backward crawl, dorsal or ventral turn, forward crawl, etc.). Brain state evolution for populations of neurons can be visualized by means of dimensionality reduction techniques, such as principal components analysis (PCA) (51). In our system, PCA was used to visualize the motor command cycle (44), which was readily observable in brain dynamics of *npr-1* animals (Fig. 5, A to D, fig. S6, and movie S2). In contrast, periods of quiescence were found to be bundled to small and confined regions between the forward and reverse motor command states (Fig. 5, B and D, fig. S6, and movie S2). Therefore, although all other motor command states feature phasic dynamics [i.e., a continuous evolution through the motor command cycle via continuously changing neuronal ensemble activities (44)], the confined bundling of principal component trajectories indicated that quiescence converged toward a fixed-point attractor. This fixed point reflects the down-regulation of many neurons but is not merely at zero in PCA space, as it is offset by the sustained activity of neurons active during quiescence, such as RIS.

Characteristic state transitions during spontaneous and evoked arousal

Next, we sought to investigate how the quiescent brain state switches to active in a spontaneous and evoked manner. Spontaneous, short-lived exits from quiescence occurred through both forward and reversal states; however, 21% O₂-evoked exits from quiescence of *npr-1* animals exclusively occurred via a reversal state (Fig. 5E). In our previous work, we described two types of reversal states named reversal 1, which occurs after long forward periods (>3 s), and reversal 2, which occurs after short forward periods. Reversals 1 and 2 are further distinguished from each other by the delay times of Ca²⁺ transients of individual neurons participating in the global brain state transitions (44). Here we describe two new types of reversal transitions, named spontaneous activating reversal and evoked reversal, which correspond respectively to spontaneous or

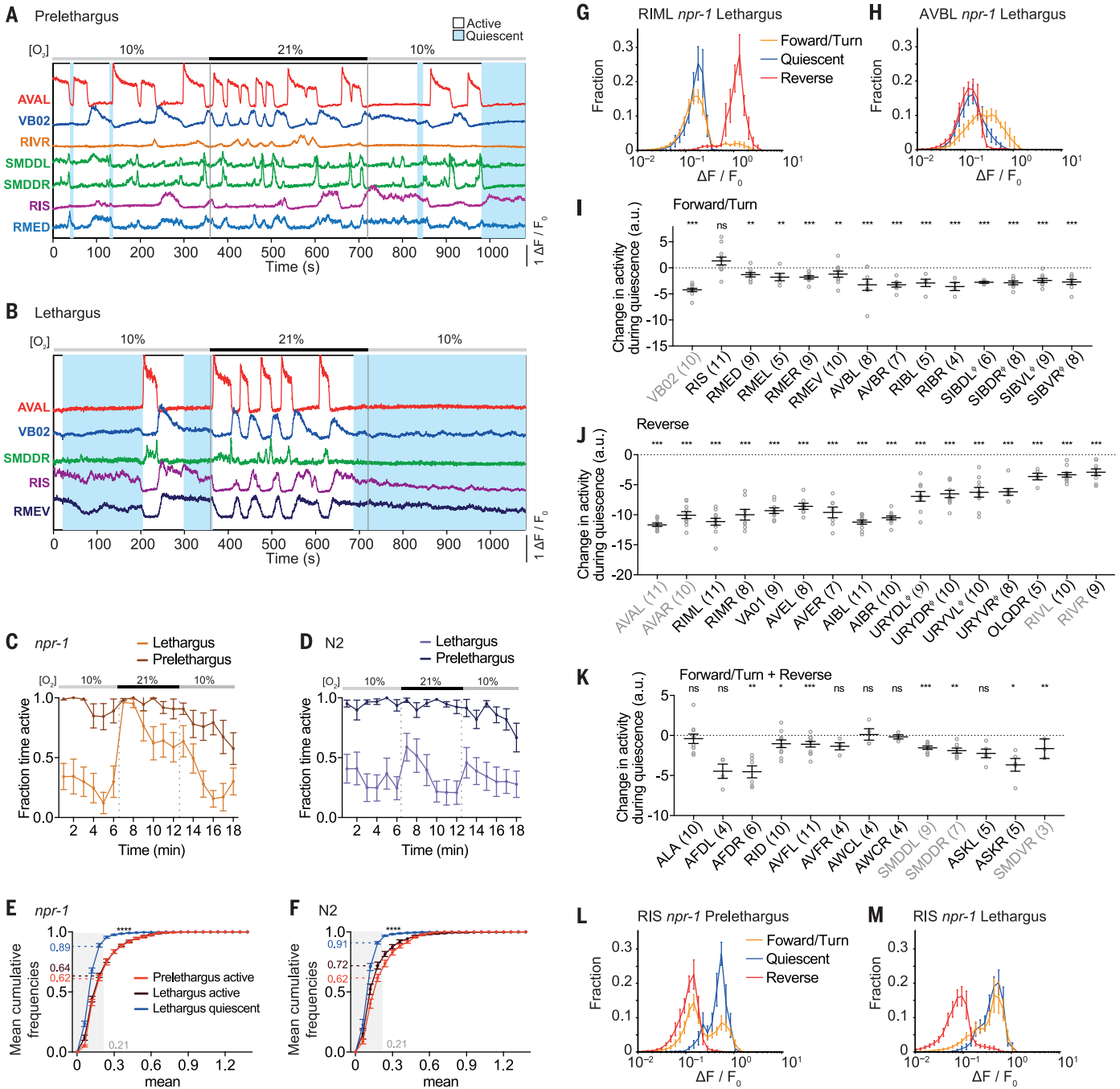


Fig. 4. Quiescent brain states have reduced activity across multiple neuron classes. Quantitative data corresponding to the brainwide imaging recordings in Fig. 3 are shown for *npr-1* (prelethargus $n = 10$, lethargus $n = 11$) and N2 (prelethargus $n = 10$, lethargus $n = 12$). (**A** and **B**) Example traces showing some of the reversal interneuron AVAL/R, the VB0 forward motor neuron SMDDL/R, and RIVL/R ventral turning neurons that are used to define quiescent (blue background) brain states (see supplementary materials for classification rules), as well as traces of the GABAergic neurons RIS and RMED/V. (**C** and **D**) Traces show mean fraction of time spent active in 1-min bins for *npr-1* (C) and N2 (D) animals. (**E** and **F**) Mean cumulative frequencies (\pm SEM) of $\Delta F/F_0$ across all neurons (excluding O₂ sensory neurons) in each recording for *npr-1* (E) and N2 (F) animals. Significant differences between lethargus active and lethargus quiescent were determined by permutation test. (**G** and **H**) Mean (\pm SEM) fractional histograms (log scale) of all measured $\Delta F/F_0$

value distributions for selected neurons during forward/turn, reversal, or quiescent brain states in lethargus: (G) RIML reversal interneuron, (H) AVBL forward interneuron. (I to K) Relative activity of the indicated neurons in the quiescent state compared to the neuron's principal state during activity, calculated as the mean difference between distributions like those shown in (G) and (H). Dots indicate difference within a single recording; bars show means \pm SEM, with N indicated in parentheses. Significance was determined by a permutation test. Neuron names shown in gray rather than black were used to classify the quiescent state. Data are from *npr-1* lethargus recordings: (I) forward/turn neurons, (J) reversal neurons, (K) all other active neurons. In (I) and (J), ambiguous neuron cell class identities are followed by ϕ ; other possible identities are shown in the supplementary materials. (L and M) RIS neuron as in (G) and (H). For all statistical tests, * $P < 0.05$, ** $P < 0.01$, *** $P < 0.001$, **** $P < 0.0001$.

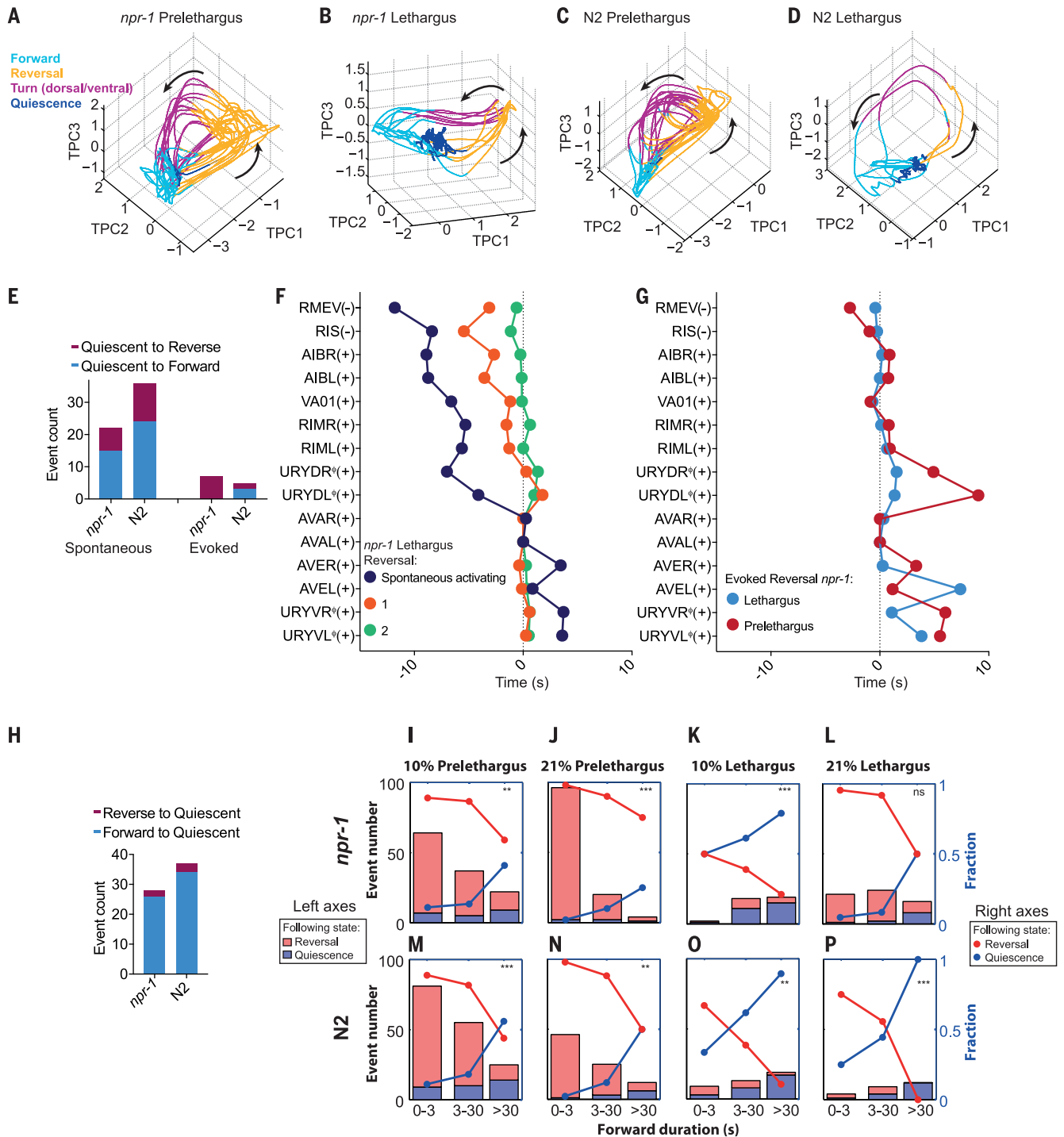


Fig. 5. Characterization of brain state transitions. (A to D) Phase plots of the first three temporal principal components (TPCs), which are the time integrals of principal components calculated from time derivatives of neuronal activity traces from brainwide imaging recordings. Developmental stage and genotype are indicated. Coloring indicates the motor command state; arrows indicate direction of trajectory. (E) Exits from quiescence bouts occur through forward or reverse brain states. “Evoked” indicates events induced by the shift to 21% O₂. (F and G) Summaries of phase timing analyses. Median phase delays of neuron classes with respect to AVAL ($t = 0$) for different reversal types are shown. Neuron polarity is designated by (+) or (-) indicating whether the neuron’s rises or falls in activity were used. The

raw data are shown in fig. S12. See table S1 for statistical analysis. Ambiguous neuron identities are denoted as in Fig. 4, I and J. (H) Quiescent brain states are frequently preceded by a forward state. (I to P) Traces (right axes) show frequency of state transitions as a function of current forward duration (time from AVA activity fall period) for *npr-1* [(I) to (L)] and N2 [(M) to (P)] for the indicated O₂ tension and developmental stage. Histograms (left axes) show number of forward periods per bin. Monotonic increases in fractions are indicated significant as determined by a permutation test; ** $P < 0.01$, *** $P < 0.001$ (see supplementary materials). Number of recordings (same as Fig. 3): *npr-1* (prelethargus $n = 10$, lethargus $n = 11$) and N2 (prelethargus $n = 10$, lethargus $n = 12$).

21% O₂-evoked events that terminate quiescence. Figure 5, F and G, summarizes results; fig. S12 shows details. Spontaneous activating reversals feature early recruitment of some neurons (e.g., interneurons AIB and RIM; head motor neuron SMDDL) but otherwise display a similar order of Ca²⁺ signals as in reversal 1 (compare Fig. 5, F and G; compare fig. S12, B and C). In contrast, evoked reversals in *npr-1* animals are rapid transitions exhibiting short phase delays between neurons, a feature shared with reversal 2 (compare Fig. 5, F and G; compare fig. S12, A and D). This observation highlights a difference between O₂-evoked responses and a previously reported nociceptive response, which during lethargus is accompanied by a decorrelation of interneuron activity (37). During evoked reversals, Ca²⁺ signals of O₂ sensory neurons URX, AQR, IL2, and URX's principal postsynaptic interneuron target AUA rose consistently earlier than all other participating neurons (fig. S12, A and E). Thus, spontaneous arousal from quiescence evolves through a characteristic sequence of neuronal ensemble activity, and O₂ sensory circuits effectively and rapidly recruit motor command activity similar to that observed in already active animals. Table S1 shows statistical tests for all relevant comparisons.

Prolonged forward states transition to quiescence

Next, we investigated how the active brain state switches to quiescence. The great majority of transitions into quiescence occurred through forward states (Fig. 5H). We calculated the fractions of reversal and quiescence transitions as a function of forward duration, which we define as the time passed since AVA activity fall (Fig. 5, I to P). Behavioral studies have shown that the duration of forward episodes decays with two exponential time constants (52, 53). We made a consistent observation with forward state durations in our immobilized preparation: In both N2 and *npr-1* prelethargus animals, most forward initiations were terminated by a reversal command within 3 s, leading to continuation of active states (Fig. 5, I, J, M, and N). In contrast, in lethargus animals the distributions of forward lengths shifted to longer durations (>3 s). Furthermore, instead of observing constant transition rates into quiescence, we observed that the fraction of forward periods ending in quiescence increased over forward state duration, thereby exceeding the fraction of reversal commands after 30 s (Fig. 5, K, L, O, and P). This was the case for both N2 and *npr-1* animals, except for *npr-1* animals experiencing 21% O₂ stimulation, where reversal command probability remained relatively high throughout the length of forward periods (Fig. 5L). These data show that quiescence entry during lethargus depends on the prior time that animals spent in the forward period and that arousing sensory cues can maintain the active brain state by triggering reversal commands, thereby resetting the system to another active period.

Our findings indicate that the low activity of the NPR-1 neuropeptide receptor in wild *C. elegans*

confers regulation of a quiescent behavioral state during lethargus in response to environmental O₂ conditions. This might be a self-protective strategy in which low O₂ could signify safer environments such as a social aggregate (37). EEG signatures define the various stages of sleep in mammals, although with low spatial resolution (14). In contrast, sleep states in invertebrates have so far mostly relied on the classical behavioral definition of sleep (19–22, 54–56); however, local field potential recordings and calcium imaging in flies show neuronal down-regulation during sleep (9, 57). Our work reveals a global neuronal signature of an invertebrate sleep state, which modulates the activity of most individual active neurons. Although active *C. elegans* exhibit phasic neuronal population dynamics that represent the motor command states (44), quiescence corresponds to a more stationary region around a fixed point in neuronal state space. This attractor feature implies that the quiescent state is an intrinsic network property and that sleep-promoting neurons and brain centers—as reported across many organisms (2, 29, 58–60)—might be integral parts of neural networks, as opposed to hierarchically organized top-down controllers. This could enable an efficient means of changing the global state of the brain via neuromodulators by subtly changing its state bias, as opposed to instantaneous reprogramming of all its individual network components. During lethargus, the quiescence attractor can thus be seen as a default state of the network that emerges in the absence of arousing inputs. Dedicated sensory circuits can rapidly switch the brain state to active by recruiting behavior-related neuronal population dynamics. Conversely, during nonlethargic phases such as prelethargus, the putative default state is maintained activity (switching among forward, reverse, and turning) regardless of the sensory input. Building on recent studies reporting the requirement for neuropeptides, we suggest that these neuromodulators are crucial for establishing the propensity for the quiescent network state during lethargus (19, 29, 49, 61–63). Therefore, global brain states are likely controlled by multiple signals antagonizing or promoting arousal and quiescence, and which originate from both the environment and the internal state of the animal.

It is possible that the quiescence brain state in *C. elegans* serves a function equivalent to the default mode in the human brain, which corresponds to intrinsic functional activity of the awake brain at rest (64, 65). Moreover, we find differences as well as parallels between mammalian deep sleep and *C. elegans* lethargus. Ensembles of cortical neurons exhibit periodic high-amplitude oscillations (delta wave) during deep sleep (10), whereas the *C. elegans* brain during lethargus nonperiodically fluctuates between quiescence and short active bouts. However, both have periods of almost complete down-regulation of neuronal activity: the trough of the delta wave oscillation in mammals (10–12) and brainwide quiescence in *C. elegans*. In addition, the short active bouts resemble micro-arousals occurring during mammalian deep sleep (12, 66). We thus provide a

neuronal imaging paradigm to study the endocrine control, network mechanisms, evolution, and basic functions of global brain states such as active wakefulness, rest, and sleep.

REFERENCES AND NOTES

1. R. Allada, J. M. Siegel, Unearthing the phylogenetic roots of sleep. *Curr. Biol.* **18**, R670–R679 (2008). doi: [10.1016/j.cub.2008.06.033](https://doi.org/10.1016/j.cub.2008.06.033); pmid: [18682212](https://pubmed.ncbi.nlm.nih.gov/18682212/)
2. C. B. Saper, P. M. Fuller, N. P. Pedersen, J. Lu, T. E. Scammell, Sleep state switching. *Neuron* **68**, 1023–1042 (2010). doi: [10.1016/j.neuron.2010.11.032](https://doi.org/10.1016/j.neuron.2010.11.032); pmid: [21172606](https://pubmed.ncbi.nlm.nih.gov/21172606/)
3. J. M. Krueger, F. Obál Jr., A neuronal group theory of sleep function. *J. Sleep Res.* **2**, 63–69 (1993). doi: [10.1111/j.1365-2869.1993.tb00064.x](https://doi.org/10.1111/j.1365-2869.1993.tb00064.x); pmid: [10607073](https://pubmed.ncbi.nlm.nih.gov/10607073/)
4. J. M. Krueger et al., Sleep as a fundamental property of neuronal assemblies. *Nat. Rev. Neurosci.* **9**, 910–919 (2008). doi: [10.1038/nrn2521](https://doi.org/10.1038/nrn2521); pmid: [18985047](https://pubmed.ncbi.nlm.nih.gov/18985047/)
5. I. N. Pigarev, H. C. Nothdurft, S. Kastner, Evidence for asynchronous development of sleep in cortical areas. *Neuroreport* **8**, 2557–2560 (1997). doi: [10.1097/00001756-199707280-00027](https://doi.org/10.1097/00001756-199707280-00027); pmid: [9261826](https://pubmed.ncbi.nlm.nih.gov/9261826/)
6. V. V. Vyazovskiy et al., Local sleep in awake rats. *Nature* **472**, 443–447 (2011). doi: [10.1038/nature10009](https://doi.org/10.1038/nature10009); pmid: [21525926](https://pubmed.ncbi.nlm.nih.gov/21525926/)
7. V. Hinard et al., Key electrophysiological, molecular, and metabolic signatures of sleep and wakefulness revealed in primary cortical cultures. *J. Neurosci.* **32**, 12506–12517 (2012). doi: [10.1523/JNEUROSCI.2306-12.2012](https://doi.org/10.1523/JNEUROSCI.2306-12.2012); pmid: [22956841](https://pubmed.ncbi.nlm.nih.gov/22956841/)
8. L. M. Mukhametov, A. Y. Supin, I. G. Polyakova, Interhemispheric asymmetry of the electroencephalographic sleep patterns in dolphins. *Brain Res.* **134**, 581–584 (1977). doi: [10.1016/0006-8993\(77\)90835-6](https://doi.org/10.1016/0006-8993(77)90835-6); pmid: [902119](https://pubmed.ncbi.nlm.nih.gov/902119/)
9. D. Bushey, G. Tononi, C. Cirelli, Sleep- and wake-dependent changes in neuronal activity and reactivity demonstrated in fly neurons using in vivo calcium imaging. *Proc. Natl. Acad. Sci. U.S.A.* **112**, 4785–4790 (2015). doi: [10.1073/pnas.1419603112](https://doi.org/10.1073/pnas.1419603112); pmid: [25825756](https://pubmed.ncbi.nlm.nih.gov/25825756/)
10. M. Steriade, D. A. McCormick, T. J. Sejnowski, Thalamocortical oscillations in the sleeping and aroused brain. *Science* **262**, 679–685 (1993). doi: [10.1126/science.8235588](https://doi.org/10.1126/science.8235588); pmid: [8235588](https://pubmed.ncbi.nlm.nih.gov/8235588/)
11. M. Steriade, I. Timofeev, F. Grenier, Natural waking and sleep states: A view from inside neocortical neurons. *J. Neurophysiol.* **85**, 1969–1985 (2001). pmid: [11353014](https://pubmed.ncbi.nlm.nih.gov/11353014/)
12. B. O. Watson, D. Levenstein, J. P. Greene, J. N. Gelinias, G. Buzsáki, Network homeostasis and state dynamics of neocortical sleep. *Neuron* **90**, 839–852 (2016). doi: [10.1016/j.neuron.2016.03.036](https://doi.org/10.1016/j.neuron.2016.03.036); pmid: [27133462](https://pubmed.ncbi.nlm.nih.gov/27133462/)
13. V. V. Vyazovskiy, K. D. Harris, Sleep and the single neuron: The role of global slow oscillations in individual cell rest. *Nat. Rev. Neurosci.* **14**, 443–451 (2013). doi: [10.1038/nrn3494](https://doi.org/10.1038/nrn3494); pmid: [23635871](https://pubmed.ncbi.nlm.nih.gov/23635871/)
14. R. E. Brown, R. Basheer, J. T. McKenna, R. E. Strecker, R. W. McCarley, Control of sleep and wakefulness. *Physiol. Rev.* **92**, 1087–1187 (2012). doi: [10.1152/physrev.00032.2011](https://doi.org/10.1152/physrev.00032.2011); pmid: [22811426](https://pubmed.ncbi.nlm.nih.gov/22811426/)
15. A. L. Loomis, E. N. Harvey, G. Hobart, Further observations on the potential rhythms of the cerebral cortex during sleep. *Science* **82**, 198–200 (1935). doi: [10.1126/science.82.2122.198](https://doi.org/10.1126/science.82.2122.198); pmid: [17844579](https://pubmed.ncbi.nlm.nih.gov/17844579/)
16. E. Aserinsky, N. Kleitman, Regularly occurring periods of eye motility, and concomitant phenomena, during sleep. *Science* **118**, 273–274 (1953). doi: [10.1126/science.118.3062.273](https://doi.org/10.1126/science.118.3062.273); pmid: [13089671](https://pubmed.ncbi.nlm.nih.gov/13089671/)
17. L. A. Finelli, H. Baumann, A. A. Borbély, P. Achermann, Dual electroencephalogram markers of human sleep homeostasis: Correlation between theta activity in waking and slow-wave activity in sleep. *Neuroscience* **101**, 523–529 (2000). doi: [10.1016/S0306-4522\(00\)00409-7](https://doi.org/10.1016/S0306-4522(00)00409-7); pmid: [11113301](https://pubmed.ncbi.nlm.nih.gov/11113301/)
18. A. Suzuki, C. M. Sinton, R. W. Greene, M. Yanagisawa, Behavioral and biochemical dissociation of arousal and homeostatic sleep need influenced by prior wakeful experience in mice. *Proc. Natl. Acad. Sci. U.S.A.* **110**, 10288–10293 (2013). doi: [10.1073/pnas.1308295110](https://doi.org/10.1073/pnas.1308295110); pmid: [23716651](https://pubmed.ncbi.nlm.nih.gov/23716651/)
19. D. M. Raizen et al., Lethargus is a *Caenorhabditis elegans* sleep-like state. *Nature* **451**, 569–572 (2008). doi: [10.1038/nature06535](https://doi.org/10.1038/nature06535); pmid: [18185515](https://pubmed.ncbi.nlm.nih.gov/18185515/)
20. S. Iwanir et al., The microarchitecture of *C. elegans* behavior during lethargus: Homeostatic bout dynamics, a typical body posture, and regulation by a central neuron. *Sleep* **36**, 385–395 (2013). doi: [10.5665/sleep.2456](https://doi.org/10.5665/sleep.2456); pmid: [23449971](https://pubmed.ncbi.nlm.nih.gov/23449971/)

21. N. Tramm, N. Oppenheimer, S. Nagy, E. Efrati, D. Biron, Why do sleeping nematodes adopt a hockey-stick-like posture? *PLoS ONE* **9**, e101162 (2014). doi: [10.1371/journal.pone.0101162](https://doi.org/10.1371/journal.pone.0101162); pmid: [25025212](https://pubmed.ncbi.nlm.nih.gov/25025212/)
22. J. Schwarz, J.-P. Spies, H. Bringmann, Reduced muscle contraction and a relaxed posture during sleep-like lethargus. *Worm* **1**, 12–14 (2012). doi: [10.4161/worm.19499](https://doi.org/10.4161/worm.19499); pmid: [24058817](https://pubmed.ncbi.nlm.nih.gov/24058817/)
23. S. Nagy et al., Homeostasis in *C. elegans* sleep is characterized by two behaviorally and genetically distinct mechanisms. *eLife* **3**, e04380 (2014). doi: [10.7554/eLife.04380](https://doi.org/10.7554/eLife.04380); pmid: [25474127](https://pubmed.ncbi.nlm.nih.gov/25474127/)
24. G. C. Monsalve, C. Van Buskirk, A. R. Frand, LIN-42/PERIOD controls cyclical and developmental progression of *C. elegans* molts. *Curr. Biol.* **21**, 2033–2045 (2011). doi: [10.1016/j.cub.2011.10.054](https://doi.org/10.1016/j.cub.2011.10.054); pmid: [22137474](https://pubmed.ncbi.nlm.nih.gov/22137474/)
25. S. Choi, M. Chatzigeorgiou, K. P. Taylor, W. R. Schafer, J. M. Kaplan, Analysis of NPR-1 reveals a circuit mechanism for behavioral quiescence in *C. elegans*. *Neuron* **78**, 869–880 (2013). doi: [10.1016/j.neuron.2013.04.002](https://doi.org/10.1016/j.neuron.2013.04.002); pmid: [23764289](https://pubmed.ncbi.nlm.nih.gov/23764289/)
26. C. Van Buskirk, P. W. Sternberg, Epidermal growth factor signaling induces behavioral quiescence in *Caenorhabditis elegans*. *Nat. Neurosci.* **10**, 1300–1307 (2007). doi: [10.1038/nrn1981](https://doi.org/10.1038/nrn1981); pmid: [17891142](https://pubmed.ncbi.nlm.nih.gov/17891142/)
27. K. Singh, J. Y. Ju, M. B. Walsh, M. A. Dilorio, A. C. Hart, Deep conservation of genes required for both *Drosophila melanogaster* and *Caenorhabditis elegans* sleep includes a role for dopaminergic signaling. *Sleep* **37**, 1439–1451 (2014). doi: [10.5665/sleep.3990](https://doi.org/10.5665/sleep.3990); pmid: [25142568](https://pubmed.ncbi.nlm.nih.gov/25142568/)
28. N. F. Trojanowski, D. M. Raizen, Call it worm sleep. *Trends Neurosci.* **39**, 54–62 (2016). doi: [10.1016/j.tins.2015.12.005](https://doi.org/10.1016/j.tins.2015.12.005); pmid: [26747654](https://pubmed.ncbi.nlm.nih.gov/26747654/)
29. M. Turek, I. Lewandrowski, H. Bringmann, An AP2 transcription factor is required for a sleep-active neuron to induce sleep-like quiescence in *C. elegans*. *Curr. Biol.* **23**, 2215–2223 (2013). doi: [10.1016/j.cub.2013.09.028](https://doi.org/10.1016/j.cub.2013.09.028); pmid: [24184105](https://pubmed.ncbi.nlm.nih.gov/24184105/)
30. J. Schwarz, I. Lewandrowski, H. Bringmann, Reduced activity of a sensory neuron during a sleep-like state in *Caenorhabditis elegans*. *Curr. Biol.* **21**, R983–R984 (2011). doi: [10.1016/j.cub.2011.10.046](https://doi.org/10.1016/j.cub.2011.10.046); pmid: [22192827](https://pubmed.ncbi.nlm.nih.gov/22192827/)
31. J. Y. Cho, P. W. Sternberg, Multilevel modulation of a sensory motor circuit during *C. elegans* sleep and arousal. *Cell* **156**, 249–260 (2014). doi: [10.1016/j.cell.2013.11.036](https://doi.org/10.1016/j.cell.2013.11.036); pmid: [24439380](https://pubmed.ncbi.nlm.nih.gov/24439380/)
32. S. Choi et al., Sensory neurons arouse *C. elegans* locomotion via both glutamate and neuropeptide release. *PLoS Genet.* **11**, e1005359 (2015). doi: [10.1371/journal.pgen.1005359](https://doi.org/10.1371/journal.pgen.1005359); pmid: [26154367](https://pubmed.ncbi.nlm.nih.gov/26154367/)
33. P. T. McGrath et al., Quantitative mapping of a digenic behavioral trait implicates globin variation in *C. elegans* sensory behaviors. *Neuron* **61**, 692–699 (2009). doi: [10.1016/j.neuron.2009.02.012](https://doi.org/10.1016/j.neuron.2009.02.012); pmid: [19285466](https://pubmed.ncbi.nlm.nih.gov/19285466/)
34. M. de Bono, C. I. Bargmann, Natural variation in a neuropeptide Y receptor homolog modifies social behavior and food response in *C. elegans*. *Cell* **94**, 679–689 (1998). doi: [10.1016/S0092-8674\(00\)81609-8](https://doi.org/10.1016/S0092-8674(00)81609-8); pmid: [9741632](https://pubmed.ncbi.nlm.nih.gov/9741632/)
35. S. Nagy, D. M. Raizen, D. Biron, Measurements of behavioral quiescence in *Caenorhabditis elegans*. *Methods* **68**, 500–507 (2014). doi: [10.1016/j.jymeth.2014.03.009](https://doi.org/10.1016/j.jymeth.2014.03.009); pmid: [24642199](https://pubmed.ncbi.nlm.nih.gov/24642199/)
36. J. M. Gray et al., Oxygen sensation and social feeding mediated by a *C. elegans* guanylate cyclase homologue. *Nature* **430**, 317–322 (2004). doi: [10.1038/nature02714](https://doi.org/10.1038/nature02714); pmid: [15220933](https://pubmed.ncbi.nlm.nih.gov/15220933/)
37. C. Rogers, A. Persson, B. Cheung, M. de Bono, Behavioral motifs and neural pathways coordinating O₂ responses and aggregation in *C. elegans*. *Curr. Biol.* **16**, 649–659 (2006). doi: [10.1016/j.cub.2006.03.023](https://doi.org/10.1016/j.cub.2006.03.023); pmid: [16581509](https://pubmed.ncbi.nlm.nih.gov/16581509/)
38. M. Zimmer et al., Neurons detect increases and decreases in oxygen levels using distinct guanylate cyclases. *Neuron* **61**, 865–879 (2009). doi: [10.1016/j.neuron.2009.02.013](https://doi.org/10.1016/j.neuron.2009.02.013); pmid: [19323996](https://pubmed.ncbi.nlm.nih.gov/19323996/)
39. I. Hums et al., Regulation of two motor patterns enables the gradual adjustment of locomotion strategy in *Caenorhabditis elegans*. *eLife* **5**, e14116 (2016). doi: [10.7554/eLife.14116](https://doi.org/10.7554/eLife.14116); pmid: [27222228](https://pubmed.ncbi.nlm.nih.gov/27222228/)
40. E. Z. Macosko et al., A hub-and-spoke circuit drives pheromone attraction and social behaviour in *C. elegans*. *Nature* **458**, 1171–1175 (2009). doi: [10.1038/nature07886](https://doi.org/10.1038/nature07886); pmid: [19349961](https://pubmed.ncbi.nlm.nih.gov/19349961/)
41. J. G. White, E. Southgate, J. N. Thomson, S. Brenner, The structure of the nervous system of the nematode *Caenorhabditis elegans*. *Philos. Trans. R. Soc. London Ser. B* **314**, 1–340 (1986). doi: [10.1098/rstb.1986.0056](https://doi.org/10.1098/rstb.1986.0056); pmid: [22462104](https://pubmed.ncbi.nlm.nih.gov/22462104/)
42. C. Rogers et al., Inhibition of *Caenorhabditis elegans* social feeding by FMRFamide-related peptide activation of NPR-1. *Nat. Neurosci.* **6**, 1178–1185 (2003). doi: [10.1038/nrn1140](https://doi.org/10.1038/nrn1140); pmid: [14555955](https://pubmed.ncbi.nlm.nih.gov/14555955/)
43. T. Schrödel, R. Prevedel, K. Aumayr, M. Zimmer, A. Vaziri, Brain-wide 3D imaging of neuronal activity in *Caenorhabditis elegans* with sculpted light. *Nat. Methods* **10**, 1013–1020 (2013). doi: [10.1038/nmeth.2637](https://doi.org/10.1038/nmeth.2637); pmid: [24013820](https://pubmed.ncbi.nlm.nih.gov/24013820/)
44. S. Kato et al., Global brain dynamics embed the motor command sequence of *Caenorhabditis elegans*. *Cell* **163**, 656–669 (2015). doi: [10.1016/j.cell.2015.09.034](https://doi.org/10.1016/j.cell.2015.09.034); pmid: [26478179](https://pubmed.ncbi.nlm.nih.gov/26478179/)
45. T. Kawano et al., An imbalancing act: Gap junctions reduce the backward motor circuit activity to bias *C. elegans* for forward locomotion. *Neuron* **72**, 572–586 (2011). doi: [10.1016/j.neuron.2011.09.005](https://doi.org/10.1016/j.neuron.2011.09.005); pmid: [22099460](https://pubmed.ncbi.nlm.nih.gov/22099460/)
46. K. E. Busch et al., Tonic signaling from O₂ sensors sets neural circuit activity and behavioral state. *Nat. Neurosci.* **15**, 581–591 (2012). doi: [10.1038/nn.3061](https://doi.org/10.1038/nn.3061); pmid: [22388961](https://pubmed.ncbi.nlm.nih.gov/22388961/)
47. H. Jang et al., Dissection of neuronal gap junction circuits that regulate social behavior in *Caenorhabditis elegans*. *Proc. Natl. Acad. Sci. U.S.A.* **114**, E1263–E1272 (2017). doi: [10.1073/pnas.1621274114](https://doi.org/10.1073/pnas.1621274114); pmid: [28143932](https://pubmed.ncbi.nlm.nih.gov/28143932/)
48. A. J. Hill, R. Mansfield, J. M. N. G. Lopez, D. M. Raizen, C. Van Buskirk, Cellular stress induces a protective sleep-like state in *C. elegans*. *Curr. Biol.* **24**, 2399–2405 (2014). doi: [10.1016/j.cub.2014.08.040](https://doi.org/10.1016/j.cub.2014.08.040); pmid: [25264259](https://pubmed.ncbi.nlm.nih.gov/25264259/)
49. M. D. Nelson et al., FMRFamide-like FLP-13 neuropeptides promote quiescence following heat stress in *Caenorhabditis elegans*. *Curr. Biol.* **24**, 2406–2410 (2014). doi: [10.1016/j.cub.2014.08.037](https://doi.org/10.1016/j.cub.2014.08.037); pmid: [25264253](https://pubmed.ncbi.nlm.nih.gov/25264253/)
50. M. Gendrel, E. G. Atlas, O. Hobert, A cellular and regulatory map of the GABAergic nervous system of *C. elegans*. *eLife* **5**, e17686 (2016). doi: [10.7554/eLife.17686](https://doi.org/10.7554/eLife.17686); pmid: [27740909](https://pubmed.ncbi.nlm.nih.gov/27740909/)
51. J. P. Cunningham, B. M. Yu, Dimensionality reduction for large-scale neural recordings. *Nat. Neurosci.* **17**, 1500–1509 (2014). doi: [10.1038/nn.3776](https://doi.org/10.1038/nn.3776); pmid: [25151264](https://pubmed.ncbi.nlm.nih.gov/25151264/)
52. R. Shingai, Durations and frequencies of free locomotion in wild type and GABAergic mutants of *Caenorhabditis elegans*. *Neurosci. Res.* **38**, 71–83 (2000). doi: [10.1016/S0168-0102\(00\)00148-6](https://doi.org/10.1016/S0168-0102(00)00148-6); pmid: [10997580](https://pubmed.ncbi.nlm.nih.gov/10997580/)
53. N. Srivastava, D. A. Clark, A. D. T. Samuel, Temporal analysis of stochastic turning behavior of swimming *C. elegans*. *J. Neurophysiol.* **102**, 1172–1179 (2009). doi: [10.1152/jn.90952.2008](https://doi.org/10.1152/jn.90952.2008); pmid: [19535479](https://pubmed.ncbi.nlm.nih.gov/19535479/)
54. J. C. Hendricks et al., Rest in *Drosophila* is a sleep-like state. *Neuron* **25**, 129–138 (2000). doi: [10.1016/S0896-6273\(00\)80877-6](https://doi.org/10.1016/S0896-6273(00)80877-6); pmid: [10707978](https://pubmed.ncbi.nlm.nih.gov/10707978/)
55. J. C. Hendricks, A. Sehgal, A. I. Pack, The need for a simple animal model to understand sleep. *Prog. Neurobiol.* **61**, 339–351 (2000). doi: [10.1016/S0301-0082\(99\)00048-9](https://doi.org/10.1016/S0301-0082(99)00048-9); pmid: [10727779](https://pubmed.ncbi.nlm.nih.gov/10727779/)
56. S. S. Campbell, I. Tobler, Animal sleep: A review of sleep duration across phylogeny. *Neurosci. Biobehav. Rev.* **8**, 269–300 (1984). doi: [10.1016/0149-7634\(84\)90054-X](https://doi.org/10.1016/0149-7634(84)90054-X); pmid: [6504414](https://pubmed.ncbi.nlm.nih.gov/6504414/)
57. D. A. Nitz, B. van Swinderen, G. Tononi, R. J. Greenspan, Electrophysiological correlates of rest and activity in *Drosophila melanogaster*. *Curr. Biol.* **12**, 1934–1940 (2002). doi: [10.1016/S0960-9822\(02\)01300-3](https://doi.org/10.1016/S0960-9822(02)01300-3); pmid: [12445387](https://pubmed.ncbi.nlm.nih.gov/12445387/)
58. M. Xu et al., Basal forebrain circuit for sleep-wake control. *Nat. Neurosci.* **18**, 1641–1647 (2015). doi: [10.1038/nn.4143](https://doi.org/10.1038/nn.4143); pmid: [26457552](https://pubmed.ncbi.nlm.nih.gov/26457552/)
59. S. Potdar, V. Sheeba, Lessons from sleeping flies: Insights from *Drosophila melanogaster* on the neuronal circuitry and importance of sleep. *J. Neurogenet.* **27**, 23–42 (2013). doi: [10.3109/01677063.2013.791692](https://doi.org/10.3109/01677063.2013.791692); pmid: [23701413](https://pubmed.ncbi.nlm.nih.gov/23701413/)
60. J. M. Donlea, D. Pimentel, G. Miesenböck, Neuronal machinery of sleep homeostasis in *Drosophila*. *Neuron* **81**, 860–872 (2014). doi: [10.1016/j.neuron.2013.12.013](https://doi.org/10.1016/j.neuron.2013.12.013); pmid: [24559676](https://pubmed.ncbi.nlm.nih.gov/24559676/)
61. M. D. Nelson et al., The neuropeptide NLP-22 regulates a sleep-like state in *Caenorhabditis elegans*. *Nat. Commun.* **4**, 2846 (2013). doi: [10.1038/ncomms3846](https://doi.org/10.1038/ncomms3846); pmid: [24301180](https://pubmed.ncbi.nlm.nih.gov/24301180/)
62. M. Turek, J. Besseling, J. P. Spies, S. König, H. Bringmann, Sleep-active neuron specification and sleep induction require FLP-11 neuropeptides to systemically induce sleep. *eLife* **5**, e12499 (2016). doi: [10.7554/eLife.12499](https://doi.org/10.7554/eLife.12499); pmid: [26949257](https://pubmed.ncbi.nlm.nih.gov/26949257/)
63. R. D. Nath, E. S. Chow, H. Wang, E. M. Schwarz, P. W. Sternberg, *C. elegans* stress-induced sleep emerges from the collective action of multiple neuropeptides. *Curr. Biol.* **26**, 2446–2455 (2016). doi: [10.1016/j.cub.2016.07.048](https://doi.org/10.1016/j.cub.2016.07.048); pmid: [27546573](https://pubmed.ncbi.nlm.nih.gov/27546573/)
64. M. E. Raichle et al., A default mode of brain function. *Proc. Natl. Acad. Sci. U.S.A.* **98**, 676–682 (2001). doi: [10.1073/pnas.98.2.676](https://doi.org/10.1073/pnas.98.2.676); pmid: [11209064](https://pubmed.ncbi.nlm.nih.gov/11209064/)
65. M. E. Raichle, A. Z. Snyder, A default mode of brain function: A brief history of an evolving idea. *Neuroimage* **37**, 1083–1090 (2007). doi: [10.1016/j.neuroimage.2007.02.041](https://doi.org/10.1016/j.neuroimage.2007.02.041); pmid: [17719799](https://pubmed.ncbi.nlm.nih.gov/17719799/)
66. P. Halász, O. Kundra, P. Rajna, I. Pál, M. Vargha, Micro-arousals during nocturnal sleep. *Acta Physiol. Acad. Sci. Hung.* **54**, 1–12 (1979). pmid: [232612](https://pubmed.ncbi.nlm.nih.gov/232612/)

ACKNOWLEDGMENTS

We thank L. Vossahl, H. Kaplan, and M. Andrione for critically reading the manuscript; members of the Zimmer laboratory for advice and discussion; M. Suplata and M. Sonntag for writing some scripts; G. Rath for IT support; and C. Bargmann for strains. Some strains were provided by the *Caenorhabditis* Genetics Center, which is funded by NIH Office of Research Infrastructure Programs grant P40 OD010440. The research leading to these results has received funding from the European Community's Seventh Framework Programme (FP7/2007-2013)/ERC grant agreement 281869 and the Research Institute of Molecular Pathology (IMP). M.Z. is supported by Simons Foundation grant 324958; T.E. was supported by a Ph.D. fellowship of the Boehringer Ingelheim Fonds. The IMP is funded by Boehringer Ingelheim. Author contributions: A.L.A.N. designed experiments, developed analytical methods, performed experiments, and analyzed data; T.E. designed and developed methods for lethargus population assays and performed initial behavioral experiments; R.L. performed aggregation assays; M.Z. designed experiments, developed analytical methods, and led the project; and A.L.A.N. and M.Z. wrote the manuscript. Raw data and codes are available upon reasonable request.

SUPPLEMENTARY MATERIALS

www.sciencemag.org/content/356/6344/eaam6851/suppl/DC1
Materials and Methods
Figs. S1 to S12
Table S1
Movies S1 and S2
References (67–79)

30 December 2016; accepted 12 May 2017
[10.1126/science.aam6851](https://doi.org/10.1126/science.aam6851)

A global brain state underlies *C. elegans* sleep behavior

Annika L. A. Nichols, Tomás Eichler, Richard Latham and Manuel Zimmer

Science **356** (6344), eaam6851.
DOI: 10.1126/science.aam6851

Neuronal basis of lethargy in worms

How does the brain switch between wakefulness and sleep? Nichols *et al.* studied this question using brain-wide Ca^{2+} imaging at single-neuron resolution in nematodes. By changing O_2 concentrations, they could rapidly switch the worms between behaviorally quiescent and active states. They observed a global quiescence brain state characterized by the systemic down-regulation of neuronal network dynamics. Signaling from O_2 sensory neurons rapidly evoked and maintained active network dynamics. Conversely, in the absence of such arousing cues, network dynamics converged into the quiescent mode.

Science, this issue p. eaam6851

ARTICLE TOOLS	http://science.sciencemag.org/content/356/6344/eaam6851
SUPPLEMENTARY MATERIALS	http://science.sciencemag.org/content/suppl/2017/06/23/356.6344.eaam6851.DC1
RELATED CONTENT	http://stm.sciencemag.org/content/scitransmed/4/161/161ra151.full http://stm.sciencemag.org/content/scitransmed/2/31/31ra33.full http://stm.sciencemag.org/content/scitransmed/4/150/150ra122.full http://stm.sciencemag.org/content/scitransmed/4/129/129ra43.full http://stm.sciencemag.org/content/scitransmed/5/179/179ra44.full
REFERENCES	This article cites 79 articles, 9 of which you can access for free http://science.sciencemag.org/content/356/6344/eaam6851#BIBL
PERMISSIONS	http://www.sciencemag.org/help/reprints-and-permissions

Use of this article is subject to the [Terms of Service](#)

Science (print ISSN 0036-8075; online ISSN 1095-9203) is published by the American Association for the Advancement of Science, 1200 New York Avenue NW, Washington, DC 20005. The title *Science* is a registered trademark of AAAS.

Copyright © 2017 The Authors, some rights reserved; exclusive licensee American Association for the Advancement of Science. No claim to original U.S. Government Works